Failure Modes of thin supported Membranes

Hendriksen, Peter Vang; Høgsberg, J.R.; Kjeldsen, Ane Mette; Sørensen, Bent F.; Pedersen, H.G.

Published in:
Advances in Solid Oxide Fuel Cells

Publication date:
2007

FAILURE MODES OF THIN SUPPORTED MEMBRANES

P. V. Hendriksen, J. R. Høgsberg, A. M. Kjeldsen, B. F. Sørensen
Materials Research Department, Risø National Laboratory, Denmark
Frederiksborgvej 399, P.O. Box 49
DK-4000 Roskilde, Denmark

H. G. Pedersen
Haldor Topsøe A/S
Nymøllevej 55
DK-2800 Lyngby, Denmark

ABSTRACT

Four different failure modes relevant to tubular supported membranes (thin dense films on a thick porous support) were analyzed. The failure modes were: 1) Structural collapse due to external pressure 2) burst of locally unsupported areas, 3) formation of surface cracks in the membrane due to TEC-mismatches, and finally 4) delamination between membrane and support due to expansion of the membrane on use. Design criteria to minimize risk of failure by the four different modes are discussed. The theoretical analysis of the two last failure modes is compared to failures observed on actual components.

INTRODUCTION

Materials exhibiting mixed ionic/electronic conductivity (MIEC's) may be used as dense membranes for gas separation purposes, for instance for oxygen production or for supply of oxygen in production of syngas by a partial oxidation route. The achievable flux through the membrane is partly limited by the resistance to the transport of the species in the bulk, and hence to reduce the cost of the technology such membranes should be as thin as possible, and an obvious reactor design is thus an ultra thin membrane on a supporting medium. The role of the support is to ensure sufficient rigidity of the component to allow handling, and to carry most of the load if the membrane reactor is subjected to pressure differences. Units with such architecture has been pursued for both solid oxide fuel cells[1, 2] and membrane reactors for syngas production. The units may be planar or tubular. Key advantages of the former being ease of manufacture and generally compact design for a given rated output. Tubular units also have a number of advantages, key ones being: 1) Ease of manufacture by extrusion. 2) Robustness to large temperature gradients in the gas flow direction (axial direction). 3) Simplicity of sealing, and finally 4) robustness to pressure differences between the two sides. Large development programs both within the field of SOFC and in the field of membrane reactors have been based on tubular units.

Whereas the central part of the device must be gas tight, in the case of SOFC to ensure high efficiency (and long lifetime), and in the case of the membrane to ensure selectivity, the support is porous to allow gas access to the membrane/electrolyte. Classical materials for SOFC electrolytes are Yttria stabilized Zirconia , Gd-doped Ceria or La-Sr-Gallates, and candidate materials for the membrane reactors could be perovskites belonging to the class $La_{1-x}Sr_xFe_{1-y}Co_yO_3$ [3,4]. Common to both devices is thus, that they rely on ceramic com-

ponents, but yet have to operate reliably, under large pressure- as well as temperature-gradients, as the electrolyte/membrane separates a fuel from an oxidant. An analysis of possible failure modes in such devices can be of relevance both in rationalising the mechanisms behind observed failures in experimental systems, but also in formulating design criteria and material requirements to allow fail safe operation.

Stresses may build up in such bi- or multi-layered devices already in the final stages of manufacturing and/or during use. If the manufacturing involves a firing step and the layers have different TEC-values, stresses will build up during cooling. During use the component will also be exposed to various stress generating loadings. Different pressure on the two sides was already mentioned, but also if a non-homogeneous temperature distribution develops, or if one of the material changes volume (e.g. due to a chemical reaction), stresses will build up. Whether detrimental or not, depends on the magnitude compared to the material strength.

The present paper discusses mechanical failure modes of thin supported tubular membranes and the derivation criteria for fail-safe design of such. The following failure modes were analyzed, and are treated in turn in the following:

1. Collapse of support tube due to external over pressure
2. Collapse of membrane over a pore due to pressure difference over the membrane.
3. Development of surface cracks in the membrane due to TEC mismatch.
4. Buckling driven de-lamination between membrane and support due to expansion on reduction of the membrane material.

Whereas case 3 is most critical at room temperature after component manufacture, cases 1, 2 and 4 are relevant under operation. Loads associated with interactions between tube and fixture are beyond the scope of the present paper. Part of the work was carried out within an EU-funded programme aiming to develop membrane reactors (CERAM-GAS)[5] to identify rationally based material requirements and to provide guidelines for focussing the effort. Much of the analysis is based on well established theory for fracture mechanics of thin planar films[6]. However, the analysis of case 4 covers also the impacts of an external pressure on this risk failure due to buckling which is to our knowledge not available in literature.

ANALYSIS AND DISCUSSION OF FAILURE MODES

Collapse of the tube.

From a balance of plant point of view it is highly advantageous for a syngas membrane to be able to sustain an overpressure on the syngas side. Similarly, for a fuel cell and an oxygen production membrane of MIEC-type, it will be advantageous/necessary, respectively, to operate with an overpressure on the air side. This gives rise to certain design requirements. If the high pressure side is on the inside of the tube and the dense membrane lies outside the support the distribution of the load over both layers relies on the interface between the two to be sufficiently strong, whereas the interface strength is unimportant if the high pressure is on the outside. Moreover, in the former case the tube will be in tension, whereas it is in compression in the latter case. Ceramics are generally much stronger in compression than in tension and hence the most benign requirements regarding component quality, layer thicknesses and material strengths are obtained if the high pressure side is on the outside of the tube.

A tubular supported membrane of thickness, h, support thickness H and diameter $D = 2R$ (See Fig. 1 B), exposed to an external pressure q will be compressed to a degree given by:

$$\varepsilon = -\frac{qR}{E_m h + E_s H} \quad , \quad \sigma_{mem,q} = E_m \varepsilon \quad , \quad \sigma_{\sup,q} = E_s \varepsilon \qquad (1, 2, 3)$$

Where σ is the radial stress and ε the radial strain., E is Young's modulus and subscripts indicate membrane or support. (Eq. 1 follows trivially from requiring force equilibrium on half the tube. Eq. 2 is Hooke's law). For a given design (h, H, R fixed) the maximum tolerable pressure will be given by the material strength ($\sigma_{mem,max}$) in compression:

$$q_{cr} \le \frac{H}{R}\frac{E_s}{E_m}\sigma_{mem,\max} \tag{4}$$

Eq. 4. can also be used to estimate the necessary support thickness for a given strength and a required pressure. However, the tolerable pressure difference may also be limited by a tube stability criterion. If the cylinder is long (L>>R) and the membrane layer thin (h<<H), the critical pressure, q_{cr}, at which the cylinder will collapse, is given by[7]:

$$q_{cr} \le \frac{E_s}{4(1-\nu_s^2)}\left(\frac{H}{R}\right)^3 \tag{5}$$

As the tolerable pressure scales with $(H/R)^3$ from the stability criterion (Eq. 5) and only with H/R for the strength criterion (Eq. 4), it will be determined by Eq. 5 for thick walled tubes (H>H*) and by Eq. 4 for thin walled (H<H*) tubes, where:

$$H^* = \sqrt{\frac{4\sigma_{mem,\max}(1-\nu_2^2)}{E_m}} \tag{6}$$

The variation in maximum tolerable pressure with tube radius is illustrated in Figure 1 for a range of different values of the support thickness.

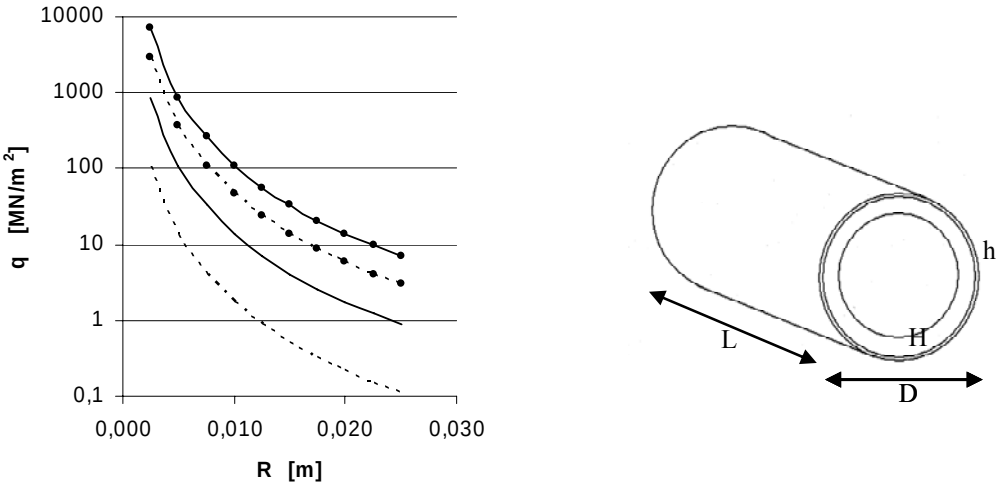

Figure 1. Calculated maximum tolerable external load (q_{cr}) on a long tube of radius R, for different wall thickness: H=0,5mm - - - , H=1mm ——— , H=1,5mm •- -• ,H= 2 mm •—•. E_s=50 GPa, ν=0,3.

Assumed values for the material constants were E_s=50 GPa, ν=0,3. (The specified value is an estimate taking into account, that the support is highly porous, which has a strong impact on the modulus[8]). Considering as an example a tube of 5 cm diameter and a required external pressure of 30 atm., the necessary support thickness deduced from the stability criterion is only 1,5 mm. Hence, the stability criterion for the above values of pressure and tube diameter does not seem to impose very stringent demands on wall thickness, and practical requirements for suitable handling strength or processes requirements are likely to require larger thicknesses. It should be noted, that in practice one would have to include certain safety factors when basing design on the above criteria; in the case of the strength criterion to take into account the spread in strengths typically observed for ceramic components due to the inherent distribution in flaw sizes, and in the case of the stability criterion (Eq. 5) to take into account geometrical imperfections like small deviation from a circular cross section which will reduce the critical load.

Collapse of the membrane over a pore or a large flaw.

As discussed in the previous section the support will relieve the stresses in the membrane due to an external pressure. However, the membrane may be left locally unsupported over large pores or other types of flaws in the interface between support and membrane. As a simple model of this situation we shall consider a thin circular plate of radius=*a* submitted to a uniform lateral load (*q*) and a uniform compression (*N*). Hence, we neglect in the model the local curvature and treat the unsupported membrane over the flaw as a flat plate. This plate problem is treated in standard textbooks[9]. Differences in the compression forces around the periphery of the plate due to the differences in the stresses in the axial and circumferential directions in the membrane are neglected. The maximum tensile stress in the plate for the present case will occur at *r=a* (at the plate periphery). It is given by:

$$\sigma_{mem,\max} = fak\frac{6M_{\max}}{h^2} - \frac{N}{h} \quad , \quad M_{\max} = \frac{1}{8}qa^2 \qquad (7, 8)$$

Where *N* is the compressive load (per unit length) acting along the outer periphery of the plate. M_{max} is the maximum moment of a plate subjected only to the lateral load, and *fak* is a "correction factor" taking into account the effect of the compression on the local curvature. It is given by:

$$fak = \frac{1-0.473\alpha}{1-\alpha} \quad \text{, where:} \quad \alpha = \frac{Na^2}{14.68D} \quad \text{and} \quad D = \frac{E_1 h^3}{12(1-\nu^2)} \qquad (9,\ 10,\ 11)$$

Here, *D* is the flexural rigidity of the plate. In the present case *N* is simply the ring stress caused by the external pressure, $\sigma_{mem,q}$ as given by Eqs. (1, 2, 3 multiplied by the membrane thickness ($N=\sigma_{mem,q}\,h$). If the external pressure gives rise only to small strains in the cylinder ($\varepsilon < 0.1(h/a)^2$), $\alpha = \varepsilon\,(a/h)^2$ will be small and *fak* close to unity, and Eqs. (7, 8 thus simplify to:

$$\sigma_{mem,\max} = \frac{3}{4}q\left\{\frac{a}{h}\right\}^2 - \frac{E_m qR}{E_m h + E_s H} \qquad (12)$$

The maximum tensile stress in the membrane over a circular flaw, calculated according to Eq. 12, is shown in Fig. 2 for a range of geometries. The curves in Fig. 2 clearly reflect that the stress is a sum of a compression, which is proportional to qR, and a tensile term due to the bending of the unsupported section of the membrane inflicted by the external pressure. The latter is also proportional to pressure, but scales with the flaw size squared. Requiring as a design criterion that the unsupported area should always be in compression the criterion between flaw-size, membrane thickness, tube size and support thickness becomes:

$$a \leq \sqrt{\frac{4E_m R}{3E_s H}}\, h \tag{13}$$

i.e. for a given flaw size, the risk of failure by this mode can be minimized by increasing the membrane thickness or by increasing the ratio between tube size and support thickness (as this increases the compressive ring stress in the membrane). The latter is of course only a sound strategy as long as one does not violate the criterion given by Eq. 4.

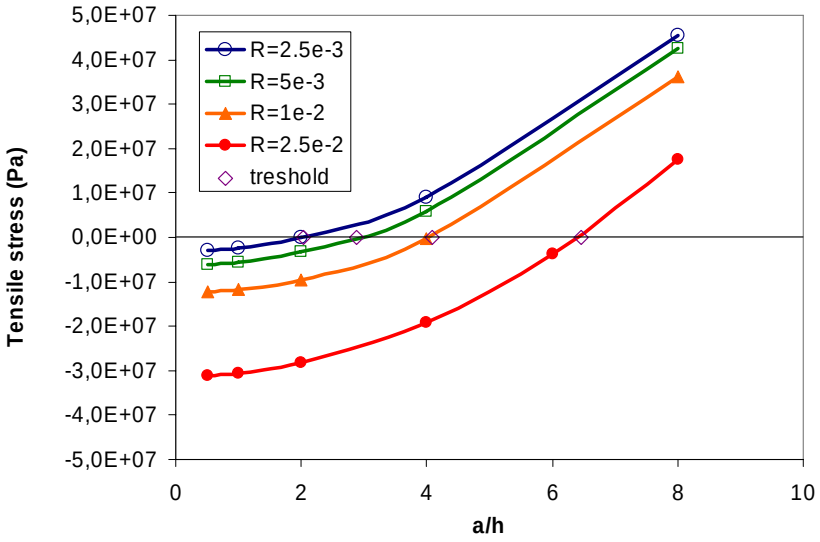

Figure 2. Maximum stress in a locally unsupported membrane plotted as a function of the flaw size for a range of tube radii (R). The pressure (q) was assumed to be 10 atm, the support thickness (H) to be 2 mm. E_s=50 GPa, h=10 µm and E_m= 125 GPa.

Also shown in Figure 2 is the $(a/h)_{crit}$ as deduced from Eq. 13 (rhombes). Evidently, the approximation fak=1 is justified for this range of parameters (The curves calculated from Eqs. 7-11 cross the axis close to the points deduced from Eq. 13). Considering as an example again a tube with R=2,5 cm, a membrane thickness of 10 µm and support thickness of 2 mm (elastic constants as stated in Fig. 1 and 2) the unsupported piece of membrane will stay in compression for flaw sizes up to a/h~6.5 or 65 µm. This is thus the tolerable size of imperfections introduced during the manufacture (measured on the length scale of the membrane thickness) before local bending of the membrane over an unsupported area introduces tensile stresses in the surface of the membrane.

Development of surface cracks due to TEC mismatches

If the difference in the thermal expansion coefficient of the membrane material and the support is too large the membrane may fail at room temperature after manufacture due to the stresses building up during cooling. Thin layers on thick supports are known in a number of technological devices and treatments of fracture mechanics in such systems can be found in literature. Evans and Hutchinson[10] have analyzed different failure modes in such systems and have shown that fail safe design criteria can be deduced from a two dimensional analysis (planar case) requiring that the energy release on failure (G) is less than the a critical material value G_c (reflecting the fracture toughness). The energy possibly released on failure is given by[4]:

$$G = \frac{h_m \sigma^2}{E_m \Omega} \leq G_c \quad , \tag{14}$$

where Ω is a cracking number (a non-dimensional constant of order unity, with small differences between different failure modes), h_m is the membrane thickness, E_m is Young's modulus of the membrane material and σ is the misfit stress in the membrane, which is simply:

$$\sigma = \frac{E_m}{(1-\nu)}\varepsilon \text{ where } \varepsilon = \Delta\alpha\Delta T. \tag{15}$$

ν is the Poisson's ratio (of the membrane material), and ε is the misfit strain which is proportional to the difference in TEC between membrane and support material times the temperature difference between the stress free state and the evaluated state (here manufacturing temperature and room temperature). Hence, when G_c is known one may use Eq. 14 to deduce a fail safe maximum layer thickness for a given misfit stress (given TEC-mismatch) or a maximum tolerable TEC-mismatch for a desired membrane thickness.

The cracking number depends on the failure mode. For the three most relevant failure modes the cracking numbers (assuming no elastic mismatch between support and film) are: 1) a surface crack, $\Omega \sim 0.25$, 2) "Channelling", $\Omega \sim 0.5$, and 3) debonding, $\Omega = 2$ [4]. By "chanelling" is meant formation of a network of surface cracks. There are a number of important things to learn from the form of Eq. 14: I) The risk of failure for all the modes scales with layer thickness, II) The risk of failure for all the modes scales with misfit-stress squared, and III) compression is preferable to tension in the membrane as the cracking number for debonding is higher than for surface cracks, which means, that under the assumption that G_c is the same for the two modes of failure, preferably the TEC of the membrane material should be lower than that of the support. However, this may not be easy to achieve in practice. Candidate membrane materials belonging to the general class $La_{1-x}Sr_xFe_{1-y}Co_yO_3$ have TEC values[11] in the range from 12 to $20 \cdot 10^{-6}$ K^{-1}(100 - 900 ^oC) strongly depending on the Sr and Co-content (increasing with both), whereas cheap strong ceramics which could be candidates for the support typically have lower TEC values. Alumina and Zirconia for instance have TEC values in the range from 8 - $11 \cdot 10^{-6}$ K^{-1} in the same temperature interval.

It follows directly from Eqs. 14, 15 that in principle large misfit stresses (large TEC-mismatches) are tolerable if one decreases layer thickness accordingly. In Table 1 design limitations in terms of allowable thicknesses for a given TEC mismatch, as well as tolerable TEC mismatch for a given membrane thickness, are assessed for a membrane relevant set of parameters. H. Lein[12] has characterised the mechanical properties of several $La_{1-x}Sr_xFe_{1-}$

$_yCo_yO_3$-perovskites and reports E-moduli in the range from 115 GPa to 180 GP, and fracture toughnesses in the range from 1.2 to 1.8 MPa $m^{1/2}$, corresponding to critical energy release rates on the order of 20 J/m^2 ($G_c \sim K_c^2/E$).

Table 1. Tolerable TEC mismatches and allowable thickness needed to ensure membrane integrity as deduced from the criterion in Eq. 14.

Parameters	Criterion
E=125 GPa, ν=0.3 ΔT=1000 Gc=20 J/m^2 h=10 μm Ω = 0.25 (surface crack)	$\Delta\alpha = \left[\Omega \frac{(1-\nu)^2}{h_m E_m} \frac{Gc}{(\Delta T)^2}\right]^{1/2} = 1\cdot 10^{-6}\ \mathrm{K}^{-1}$
As above but: Δα=5·10^{-6} K^{-1}	$hc = \Omega \frac{(1-\nu)^2}{E_m} \frac{Gc}{(\Delta\alpha\Delta T)^2} = 1.5\mu m$

The temperature difference between processing- and room-temperature may be larger than 1000 ^oC, but at these temperatures creep rates are very high for the analysed type of materials which may effectively relax the stresses.

There is of course some uncertainty on the above used parameter values, however the deduced numbers in the above examples show that this mode of failure inflicts very serious limitations in the number of possible material combinations as well as harsh requirements to the tube geometry (membrane thickness). The TEC mismatch between alumina and typical $La_{1-x}Sr_xFe_{1-y}Co_yO_3$-perovskites, which is in a very conservative estimate 5·10^{-6} K^{-1}, calls for very thin layers (below 1.5 μm) which would certainly be difficult to make in the desired quality using cheap ceramic manufacturing routes. For thicknesses in the range from 10 to 20 μm, which can be readily made[13], the required degree of TEC-matching (~1·10^{-6}) strongly limits the degrees of freedom in tuning the membrane composition to optimise other relevant properties like ionic conductivity or catalytic activity.

Experimental experiences.

Within the framework of the "CERAM-GAS" project experimental bi-layer membranes with several different material combinations were manufactured. SEM micrographs of a subset of the investigated material combinations are shown in Figure 3. The TEC mismatch between membrane material decreases from upper left to lower right in the figure (see caption). Evidently, surface cracks are observed for three (A, B, C) out of the four depicted material combinations (see the zoom-in insert on 3 B). From the limited opening of the cracks, the observed pattern (Fig. 3A) as well as the observed trans-granular tracks (Fig. 3 B) it seems evident that the cracks do not originate from imperfect application of the layer, but are due to the above described failure mode related to the TEC differences. For the successful combination in the lower right corner the TEC mismatch was ~0.1·10^{-6} K^{-1}. Note, that cracks are also observed in the case where the TEC differed by about 1.6·10^{-6} K^{-1}, which is close, but yet above, the formulated criterion. Many more material combinations than the four de-

picted in Fig.3 were investigated in the project. All successful combinations were consistent with the criterion in Table 1. (The uncertainty on the TEC measurement is ~0.1 10^{-6} K^{-1})

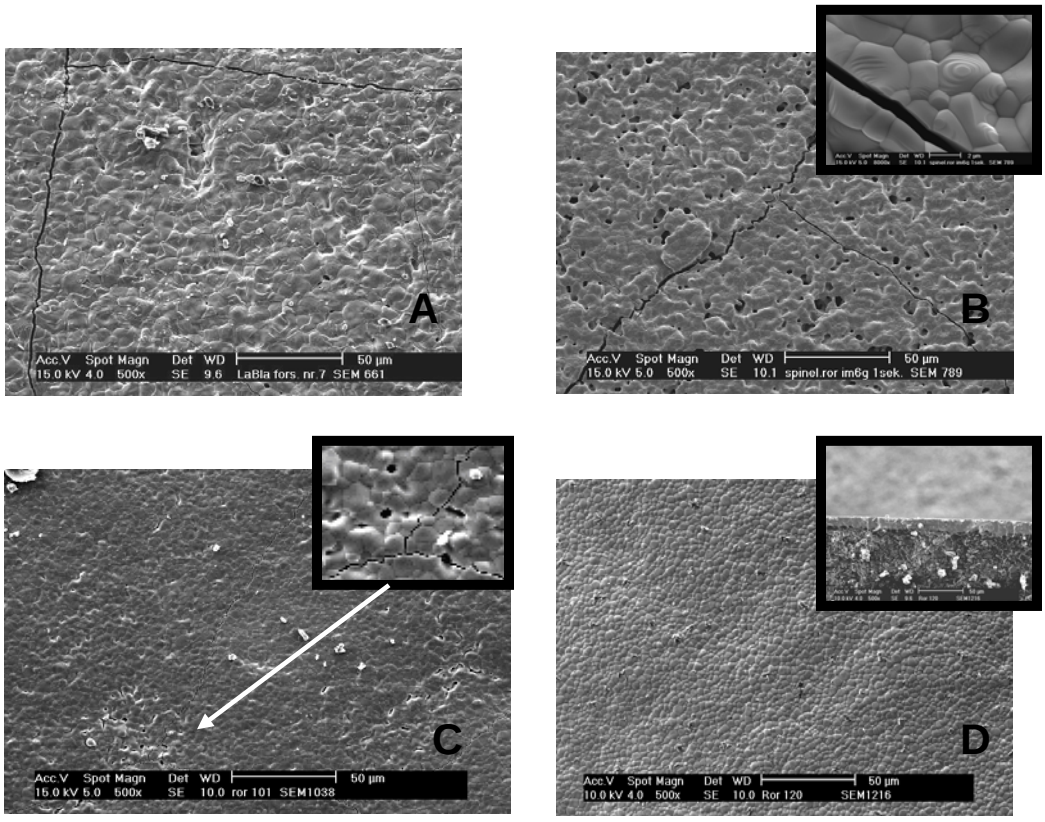

Figure 3 Top views (SEM) of different experimental supported membranes. The pictures are from different combinations of membrane material and support. A) $\Delta\alpha \sim 5 \cdot 10^{-6}$ K^{-1}, B) $\Delta\alpha \sim 4 \cdot 10^{-6}$ K^{-1}, C) $\Delta\alpha \sim 1.6 \cdot 10^{-6}$ $K^{-1}$and D) $\Delta\alpha \sim 0.1 \cdot 10^{-6}$ K^{-1} (insert shows a cross section).

Material expansion on reduction

It is a characteristic of materials showing high mixed conductivity (both oxide ions and electrons) that they are non-stoichiometric in oxygen, i.e. there is a considerable concentration of vacancies in the lattice. The concentration of vacancies depends on the surrounding oxygen activity. When such materials are used as membranes, where they are exposed to different oxygen activities on the two sides, a vacancy concentration profile will be established inside the material, the detailed shape of which depends on the membrane thickness as well as the rates of the oxygen exchange processes on the two surfaces[3]. In general there is a volume change associated with a change in vacancy concentration in the material – the materials expand on reduction[3,14,15,16] This is illustrated in Fig. 4, where measured expansions on reduction of a well characterized perovskite as well as for two membrane materials investigated in the CERAM GAS project are plotted versus the oxygen non-stoichiometry. Evidently, the strains associated with these stoichiometry changes are quite large (~0.3 – 0.4 %), and they are well known to lead to a number of mechanical problems for the use of such materials[4,15].

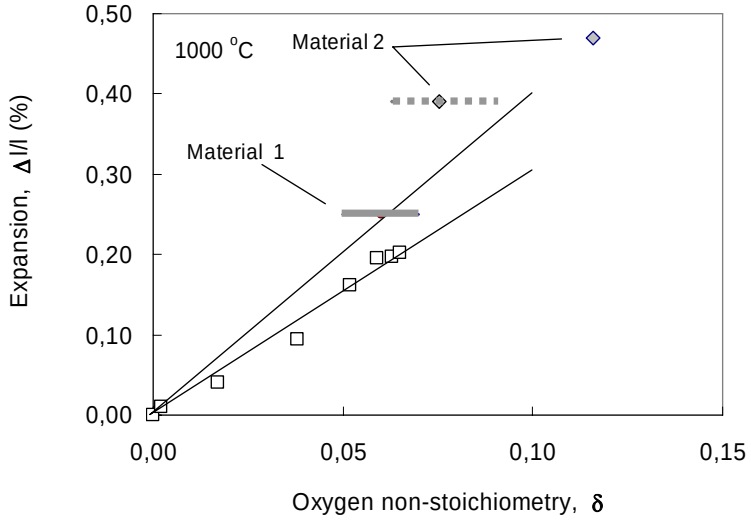

Figure 4. Measured expansions for $La_{0.8}Sr_{0.2}Cr_{0.87}Fe_{0.1}V_{0.03}O_{3-\delta}$ (squares)[16] and two materials analyzed within the CERAM-GAS project plotted versus the oxygen non stoichiometry in the materials. For two of the three measurements the oxygen activity was not measured accurately giving rise to uncertainty on the δ-values, as indicated with the horizontal bars. The upper straight line was deduced from the relation between δ and Δl/l for $La_{0.8}Sr_{0.4}Fe_{0.8}Co_{0.2}O_{3-\delta}$[14,3]

For the present application where the membrane material is in the form of a thin layer on a thick support, they will give rise to large compressive stresses in the membrane, which may if the exceed the compressive strength of the material lead to failure. Moreover, they may result in a detachment between the membrane and the support as the stresses can be relaxed if the membrane buckles away from the support (whereby it increases its length decreasing the stress level). The situation is illustrated in Fig 5. In the following we shall analyze the implications of the buckling mode of failure (The risk of failure due to excessive compressive stresses, or other than buckling driven failures in compression[17], are not addressed further in this paper, but may indeed be relevant for this type of components).

Model of buckling driven de-lamination

Buckling driven delamination between a thick support and a thin surface film in compression has been analyzed in literature, (see the paper by Hutchinson and Suo and references therein) for the case of planar geometries. Starting from this analysis J. Høghsberg[18] has generalized the treatment to take into account the cylindrical shape as well as the effects of external overpressure. Buckling driven delamination on tubular geometries has also been treated by Storåkers et al.[19,20] and J.W. Hutchinson[21]. The situation is illustrated in Fig. 5.

Describing a segment of the membrane as a beam of constant stiffness, the differential equation describing the shape of the membrane becomes:

$$w''''+k^2(w+w_0)''-\frac{q}{EI}=0\,,\quad \mathrm{k}^2=\frac{\sigma h_m}{E_m I} \tag{16}$$

Where *w(y)* is the vertical displacement, *k* is a parameter and ()' signifies the partial derivative with respect to *y*. w_o(y) is a curve describing the initial shape. E_m is Young's modulus and *I* the moment of inertia. σ is the normal stress in the beam.

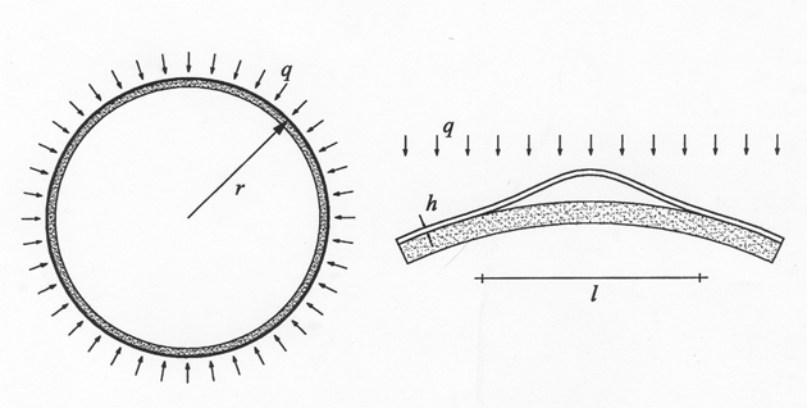

Fig. 5 Buckling of non-planar membrane subjected to external pressure (*q*) and additional in plane compression due to expansion of the membrane material.

In the considered case, the normal stress in the beam is the sum of the ring stresses, σ_r due to *q* (Eq. (1, 2, 3) and the stresses caused by the expansion of the material, σ_{exp}:

$$\sigma_t = \sigma_{\exp} + \sigma_q \approx \frac{E_m}{1-\nu}\varepsilon_{\exp} + \frac{qR}{H}\frac{E_m}{E_s} \tag{17}$$

We shall approximate the initial circular shape with a sinus function over the angular segment *l/2πR*:

$$w_0 = a_0 \sin(\frac{\pi y}{l}) \ , \tag{18}$$

which is a fair approximation for *l/R*<0,5, as this greatly simplifies the solution of Eq.16.

Under the boundary conditions *w*(0)=*w*'(0)=*w*(l)=*w'(l)*=0 (clamped ends) the solution to Eq.16 can be written:

$$w\ (y) = \left(\frac{\pi}{lk}\alpha - \frac{l}{k}\beta\right)(C(1-\cos(ky)) - \sin(ky)) + \alpha\sin(\frac{\pi}{l}y) - \beta y(1-y)\,, \tag{19}$$

$$C = \frac{kl\cos(kl) - 2\sin(kl) + kl}{2(\cos(kl)-1) + kl\sin(kl)}, \quad \text{and} \quad \alpha = \frac{a_0}{\left(\pi/lk\right)^2 - 1} \ \text{and} \ \beta = \frac{q}{2EIk^2}\,. \tag{20}$$

The energy release rate, G, may be calculated from the expression:

$$G = \frac{6l}{\overline{E}h_m^3}\left(M_l^{\,2} + \frac{h^4}{12}\Delta\sigma^2 \right), \tag{21}$$

where $\Delta\sigma$ is the reduction of the normal stress in the beam due to the buckling. The Moment M_l is related in to the second derivative of the displacement and the stress reduction to the elongation introduced on the buckling:

$$M_l = M(l) = -Elw''(l) \quad \text{and} \quad \Delta\sigma = \frac{\overline{E}_m}{2l}\int_0^l w'\,dy\,, \tag{22}$$

Where $\overline{E} = E/(1-\nu^2)$. Finally, note that the stress in the layer "during" buckling can be expressed:

$$\sigma = \sigma_t - \Delta\sigma \tag{23}$$

Equations 19 and 21 define (via Equations 17, 20, 22, and 23) a set of equations in the variables w and σ. The system may be readily solved numerically in an iterative manner and the energy release rate of the buckling calculated. A set of model results are presented in Fig. 6, illustrating the impact of parameter variations around a base case defined in the figure caption.

A number of points, relevant for materials development and design of supported membranes may readily be deduced form the results in Fig. 6:

- A certain critical membrane thickness exist in all cases, where the risk of failure is maximal. Increasing the thickness relative to this reduces the energy release rate (buckling becomes less effective for releasing the stresses) as does a decrease in thickness (less energy in the system all together). The most critical thickness is slightly thicker for the cylindrical membranes than for the planar case. The results give rather direct guidelines on how to design the membrane reactor for minimizing the risk of failure.
- The curvature of the membrane increases the risk of failure relative to the planar case i.e. G is larger for the tubular case than for the planar for a given set of parameters (Fig. 6 A).
- G_{max} (the risk of failure) increases with the lattice expansion induced strain squared, and for the base case of 0.3 %, which is not an unrealistic value (c.f. Fig. 4) G reaches a value of ~10 J/m^2. Whereas for tough perovskite materials one may expect higher values (see section on TEC-mismatches) Lein also reported toughness values on the order of 1 MPam$^{1/2}$, for some of the investigated perovskites, which corresponds to ~ 8 J/m^2 (assuming $G_c = K_c^{\,2}/E$, mode I crack opening). Moreover, for this mode of failure it is the toughness of the interface that matters, and this may well be lower than for any of the two materials of the bilayer[22]. Thus, this mode of failure may indeed be critical and put limitations to both which materials are applicable and how the reactor can be designed. Note, that relaxation by creep, which may be significant at high temperature, will alleviate the situation and thus the material requirements deduced

from this mode of failure, as will taking into account tensile residual stresses in the film at the operating temperature.

- G is also sensitive to the flaw size (see Fig. 6 C). It increases with the flaw size. In the investigated range of parameters G_{max} scales with the flaw size in a parabolic manner, and hence controlling the flaw size is effective for minimizing the risk of failure. Also the most critical thickness increases with flaw size. With "small" flaws (l=200 μm) the base case of a 10 μm thick membrane exhibits a very small G value. (Note, that for this mode of failure poor local adhesion between membrane and support is "a flaw", whereas for the local burst over areas where the membrane is unsupported "a flaw" is a missing part of material in the support).
- Finally, the effect of an external over pressure is illustrated in Fig. 6 D. Evidently, a slight overpressure is very effective for decreasing G and thus the risk of failure by this mode.

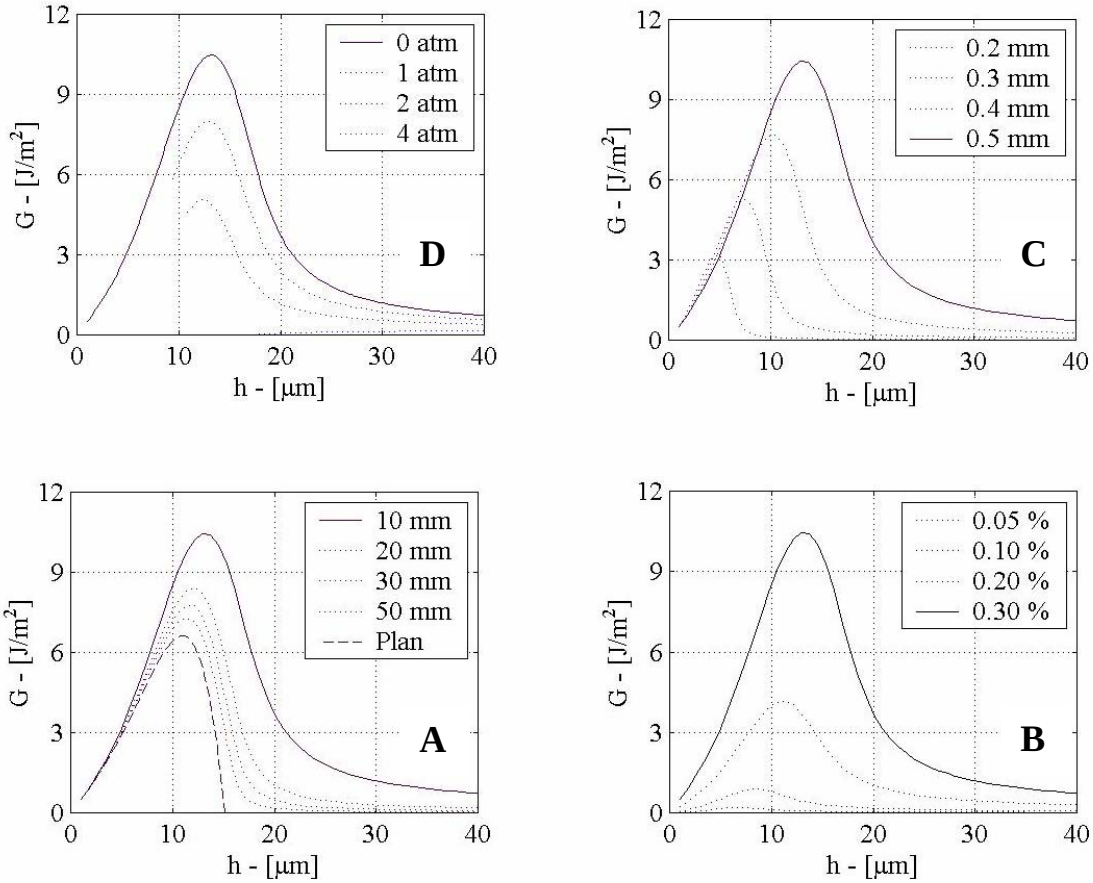

Figure 6. Calculated energy release rates for buckling driven delamination between membrane and support as a function of membrane thickness. The four figures illustrate the dependence on key parameters. A) Shows the impact of tube radius (parameter values given by the legends). B) Illustrates the impact of the membrane strain (ε_m), C) Illustrates the effects of flaw size (l), and D) the effects of external overpressure (q). The base case values of the parameters were q = 0 atm., ε_m=0,3%, E_m=100 Gpa, E_s =10 GPa, R =10 mm, l=0,5 mm, H=1 mm

Figure 7 shows an experimental membrane reactor after test, where the membrane layer has partly peeled off. It is likely that this piece failed due to a buckling driven delamination.

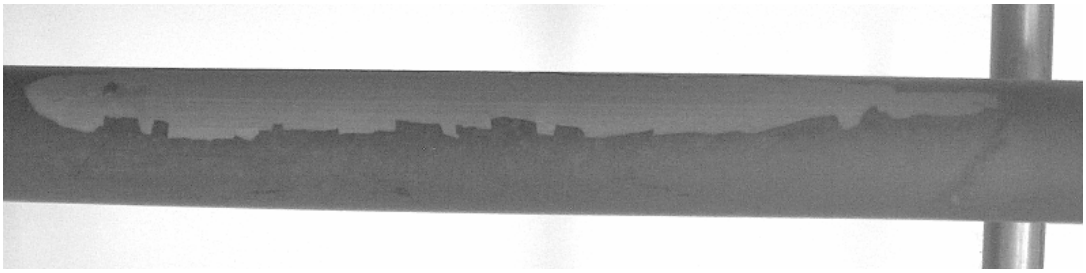

Figure 7. A section of an experimental membrane reactor that after test showed detachment between membrane and support. The reactor was prepared and tested within the framework of the CERAMGAS project.

CONCLUSION

Out of the four analysed failure modes the two ones regarding strain mismatches between membrane and support arising either from differences in TEC between the two materials or from the expansion on reduction of the membrane material were found to be the most critical. It seems likely that by proper design and careful manufacture to limit the inherent flaw size, both tube collapse and burst of local unsupported areas can be avoided for a range of technologically relevant pressures.

To avoid crack formation in the membrane on cooling after the firing step requires either extremely thin membranes or very close TEC matching between the layers. For the considered parameter values (a membrane thickness of 10 -20 μm and a TEC of the membrane exceeding that of the support) a TEC-matching of better than $1 \cdot 10^{-6}\ K^{-1}$ was postulated necessary on the basis of the fracture mechanical analysis. Experimental experience form manufacture of tubular supported membranes in several different material combinations, though not sufficiently numerous to establish the criterion accurately, was consistent with this threshold.

To avoid delamination by buckling due to the expansion of the membrane material imposes quite tough criteria on the dimensional stability of the membrane material and/or to the tolerable flaw size in the component. In the analysis of this case, the treatment of buckling driven delamination of a thin layer on a thick planar support was modified to describe also the case of a tubular support under external pressure. Like for the planar case two “safe” regimes exist in the limit of very thin and very thick membranes. The most critical thickness is increased relative to the planar case. Further, applying an external over pressure was found to a have great stabilizing effect towards this mode of failure. A failure observed on an experimental membrane was tentatively ascribed to this failure mode.

ACKNOWLEDGEMENTS

Financial support from EU via the CERAM GAS project contract G1RD-CT-1999-00023 is acknowledged. Dr. Luca Basini, Snamprogetti is acknowledged for providing photographic documentation of a failure observed on a tested reactor, and Dr. D. Lybye, Risø, for carrying out measurements of the expansion on reduction of the materials.

REFERENCES

[1] D. Stöver, H. P. Buchkremer and J. P. P. Huijsmans in "Hand book of Fuel Cells – Fundamentals, Technology and Applications" Ed. by W. Vielstich , H. A. Gasteiger, A. Lamm, Vol 4, Chap. 72. John Wiley & Sons, (2003).

[2] S. C. Singhal, "Advances in SOFC Technology", *Solid State Ionics* **135** 305-313 (2000).

[3] P.V. Hendriksen, P.H. Larsen, M. Mogensen, F.W. Poulsen and K. Wiik "Prospects and problems of dense oxygen permeable membranes", *Catal. Today* **56** 283 (2000).

[4] H.J.M. Bouwmeester, *Catal. Today* **82** 141-150 (2003).

[5] EU-project "CERAM GAS", contract G1RD-CT-1999-00023, See CORDIS http://ica.cordis.lu

[6] J. W. Hutchinson and Z. Suo, *Adv. Appl. Mech.* **29**, 63-191 (1992).

[7] S. P. Timoshenko, J.M. Gere, "Theory of elastic stability" McGraw-Hill, 1961.

[8] N. Ramakrishnan and V. S. Arunachalam, *J. Am. Ceram. Soc.* **76** 2745 (1993).

[9] S. Timoshenko, S. W.-Krieger, "Theory of Plates and Shells", McGraw-Hill, 1959.

[10] Evans and Hutchinson *Acta Metall. Mater* **43** (7) (1995).

[11] L. W. Tai, M. M. Nasrallah, H. U. Anderson, D. M. Sparlin and R. Sehlin, *Solid Stae Ionics,* **76**, 259 (1995).

[12] H. Lein "Mechanical properties and phase stability of oxygen permeable membranes, $La_{0.5}Sr_{0.5}Fe_{1-x}Co_xO_3$", Ph.D-thesis, IUK-thesis 114, imt-report 2005:69, Dep. of Mat. Tech. NTNU. 2005.

[13] N. Christiansen, S. Kristensen, H. Holm-Larsen, P. H. Larsen, M. Mogensen, P. V. Hendriksen and S. Linderoth, p. 168 in SOFC-IX, ed. by S. C. Singhal and J. Mizusaki, ECS Proc. Vol. **2005-07**. The Electrochemical Society (2005).

[14] J. W. Stevenson, T. R. Armstrong, L. R. Pedersen and W. J. Weber, Proc. of first int. symposium on ceramic membranes, ed. by H. U. Anderson, A.C. Khandkar, M. Lieu, The Electrochemical Soc. **PV 95-24,** p. 94 (1995).

[15] P.V. Hendriksen, J.D. Carter and M. Mogensen "Dimensional instability of doped lanthanum chromites in an oxygen pressure gradient", In: Proceedings of the fourth international symposium on solid oxide fuel cells (SOFC-IV), M. Dokiya, O. Yamamoto, H. Tagawa and S.C. Singhal (eds), Vol 95-1 p. 934 – 943 (1995).

[16] P.V. Hendriksen, J. Høgh, J.R. Hansen, P.H. Larsen, M. Solvang, M. Mogensen and F.W. Poulsen "Electrical conductivity and dimensional stability of Co-doped lanthanum chromites", Fifth International Symposium on Ionic and Mixed Conducting Ceramics, eds. T.A. Ramanarayanan, Y. Yokokawa and M. Mogensen, The Electrochemical Society, 2004.

[17] H. E. Evans, "Stress effects in high temperature oxidation of metals", *Int. Mat. Reviews*, **40,** 1**,** (1995)

[18] J. Riess Høgsberg. *J. Danish Ceramic Society*, **4,** (1) (ISSN 1398-3261) 2001.

[19] B. Storåkers K. F. Nielsson, "Imperfection Sensitivity at Delamination Buckling and Growth" *Int. Jour. of Solid. Struc*. **30** 1057 (1993).

[20] B. Storåkers, P. L. Larsson and C. Rohart, "On delamination Growth in Shallow Shells", *J. Appl. Mech.* **71,** 247 (2004).

[21] J. W. Hutchinson "Delamination of compressed films on curved substrates", *J. Mech and Phys. Solids* 49 1847 (2001).

[22] Sørensen, B. F., and Horsewell, A., "Crack growth along interfaces in porous ceramic layers", *J. Am. Ceram. Soc*., Vol. 84, pp. 2051-9 (2001).